Journal of Hazardous Materials 221–222 (2012) 109–117

Contents lists available at SciVerse ScienceDirect

Journal of Hazardous Materials

journal homepage: www.elsevier.com/locate/jhazmat

Characterization of mass transfer of lower chlorinated benzenes from contaminated sediment into water

Marti C. Blad[a], M. Teresa Gutierrez-Wing[b,*], W. David Constant[a]

[a] Louisiana State University, Department of Civil and Environmental Engineering, 3418 Patrick F. Taylor Hall, Baton Rouge, LA 70803, United States
[b] Louisiana State University, Department of Civil and Environmental Engineering, 116 Engineering Lab Annex (ELAB), Baton Rouge, LA 70803, United States

ARTICLE INFO

Article history:
Received 25 September 2011
Received in revised form 2 April 2012
Accepted 7 April 2012
Available online 13 April 2012

Keywords:
Chlorinated benzenes
Chemical kinetics and equilibrium
Modeling
Sediment–water transfer

ABSTRACT

Mass transport of chlorinated benzenes as found at the Petro-Processors of Louisiana, Inc. (PPI) Superfund site was characterized for a range of flow rates in small streams. At this site hazardous waste was historically disposed of in unengineered pits. Hexachlorobenzene and lesser chlorinated degradation products were found among other compounds. As waste was being disposed into unengineered pits, it seeped to lagoons and sediments of Baton Rouge Bayou (BRB), which flows through and nearby the former disposal areas. Characterization of the transport and fate of chlorobenzenes at PPI is an integral part of the Monitored Natural Attenuation (MNA) remedy currently underway. Laboratory experimental results and mathematical model predictions of the flux of 1,3-dichlorobenzene (1,3-DCB) from sediments into water are presented. 1,3-DCB was studied as individually and as part of a mixture of four contaminants with 1,2-DCB, chlorobenzene (MCB) and trichlorobenzene (TCB).

Surficial sediments were collected, spiked with contaminants and leached to determine flux over time. Two advection–dispersion models were tested and the effect of low, cycling and fast stream flow on the contaminant flux was assessed. Model results suggest that tortuosity and effective diffusivity are related effective system predictors and descriptors. Statistical analysis supports the models' predictive capabilities.

1. Introduction

At the Petro-Processors of Louisiana, Inc. (PPI) Superfund site hexachlorobenzene (HCB) is one of the principal contaminants. The degradation products of HCB include chlorobenzenes (MCB), dichlorobenzenes (DCB) and trichlorobenzenes (TCB). The PPI site is located north of Scotlandville, in East Baton Rouge Parish, Louisiana, about ten miles north of Baton Rouge. There are two disposal areas in this 55-acre site, the Scenic site, near Baton Rouge Bayou (BRB), and the Brooklawn site north of Devil's Swamp. It has been estimated that 320,000 tons of petrochemical waste were placed in the site(s) over its history (1960s and 1970s). Chlorinated organics and polycyclic aromatic hydrocarbons are the main pollutants [3,4]. The nearest community to this site is a few houses, 300 m from the border of the Scenic site. A drinking water well is located 900 m up-gradient of this site.

The remediation strategy has been hydraulic containment and recovery techniques with monitored natural attenuation (MNA) now the primary focus [1]. MNA relies on natural in situ degradation processes for the reduction of the contaminants [2–5].

A physical flux model of Baton Rouge Bayou/Devil Swamp sediments was considered to assess the fate and transport of the contaminants and movement into surface water streams. For the laboratory experiment, under different flow conditions, the flux of single and multiple contaminants was measured. These data estimated the pollutant release rates scaled to known stream flows in Baton Rouge Bayou. For this purpose an advection–dispersion model was proposed using the MATHCAD® software package. The mathematical model developed was based on a previous analytical model proposed by Choy and Reible [6] modified using laboratory experimental data analysis. Both the BRB and the Brooklawn site contain HCB and degradation products of interest in this study. However, due to historical losses of material into BRB around the Scenic site, the transport of contaminants in the BRB water column was of interest to aid in determining if active or passive remedies would be needed in the future.

Very rarely do natural systems contain a single contaminant, but for experimental purposes the laboratory model flux studies first contained a single contaminant, 1,3-dichlorobenzene (1,3-DCB). Later a mixture of four components, chlorobenzene (MCB), 1,2-dichlorobenzene (1,2-DCB), 1,3-dichlorobenzene (1,3-DCB) and

* Corresponding author. Tel.: +1 225 578 5703; fax: +1 225 578 9162.
E-mail address: mgutie5@lsu.edu (M.T. Gutierrez-Wing).

0304-3894/$ – see front matter © 2012 Elsevier B.V. All rights reserved.
http://dx.doi.org/10.1016/j.jhazmat.2012.04.014

Table 1
Soil characteristics for chlorinated benzene studies. PPI-1–5 represent the soil samples identification.

Parameter	PPI-1	PPI-2	PPI-3	PPI-4	PPI-5
pH	7.8	6.5	7.3	6	7.4
Na (ppm)	11	33	49	38	29
Mg (ppm)	50	278	347	285	197
Ca (ppm)	757	1437	3172	1625	1970
P (ppm)	55	171	264	220	162
K (ppm)	29	76	139	78	74
OM (%)	0.02	0.46	0.55	0.52	0.29
Sum bases	4.3	9.8	19.3	10.8	11.8

1,2,4-trichlorobenzene (TCB) were used for the laboratory model flux experiments.

The compounds utilized in this work, being degradation products of HCB [7–9], are more mobile than the parent compound in sediment/soil systems, and hence of environmental concern [8,10]. In the final analysis, the mathematical model uses effective diffusivity (D_e; [11]) to describe transport of lower chlorinated benzenes. The related tortuosity parameter is also investigated as a system predictor. These modeling efforts were secondary in assessment of actual chemical concentrations found in the field, but necessary to understand the impact of mixtures and flow on the flux into the water column.

2. Materials and methods

2.1. Sediment collection

Multiple surficial sediment samples were collected from BRB around the Scenic site of PPI. These sediments were sealed until they were prepared for analysis. Samples were sent to the Agronomy Laboratory at Louisiana State University where the sediment characterization parameters for five different sampling areas (PPI-1–5; Table 1) were obtained.

2.2. Sediment preparation

Sediment containers with a volume of 18.9 L (five gallon plastic buckets) were unsealed and debris was removed by hand after pouring out the sediment onto a 45.7 cm × 63.5 cm (18 in. × 25 in.) Nalgene® tray. The sediments were air dried after placing them in a hood and sieved through a #10 mesh screen. Hard clumps were removed and then ground in a grinder for homogenization. Samples were then transferred into 1 kg glass jars with Teflon® lined lids. A total of 4.5 kg of sediments were placed into jars and saturated using distilled water.

Selected sediment samples were then spiked to a desired contamination level of approximately 15 mg/kg. A 5 mg/kg level of contamination was included in the 15 mg/kg level as a safety measure against volatilization during sediment loading, transfer and mixing. The level of contamination was representative of site conditions and ensured accurate analytical results. The chlorinated benzene contaminant of interest was solubilized in methanol and then added to the sediment.

2.3. Sheet flow leaching bed (SFLB) set-up

Jars of sediment were placed in a tumbler for about 48 h in order to evenly distribute the chemicals in the spiked samples. Then the jars were emptied into a Nalgene® tray and mixed again. Two parallel SFLBs were set up as shown in Fig. 1. Contaminated sediment slurry was introduced into each bed and the beds were thumped against a table to eliminate air pockets and also to help the mixture settle. The addition of the slurry mixture continued until the top surface was even with the weirs at both ends of the beds. These weirs help in forming a 2–3 mm water column depth in laminar flow water during experiments. The sediment in the beds was smoothened to create a uniform surface. Distilled water was pumped from a reservoir via Tygon® tubing with 1/8 in. inner diameter, 3/16 in. outer diameter and 1/32 in. wall thickness, into the SFLB inlet using a multi-channel peristaltic pump. The water was initially pumped over the sediments until the area between the weirs held 2 mm of water. For about 8–16 h the water was allowed to remain in contact with the sediment. This helped in achieving initial sediment–water equilibrium. Using the same water source and parallel pumps, duplicate beds were run for each of the experiments. Flow rate was scaled to simulate channel flows typical in BRB at the site [2].

Initially, a continuous flow rate of water was used to simulate steady stream flow. Later observations were under different cycling flow rates of water to quantify contaminant removal in a dynamic environment. Three flow regimes were used for the chlorinated benzene studies. Continuous fast flow with Q = 150 mL/h, continuous slow flow with Q = 50 mL/h and a cyclic flow regime which constitutes a fast flow for 24 h and slow flow for 24 h. Continuous flow helps in determining flux rate and steady state chlorinated benzene concentrations. Cyclic flow prevents the system from achieving equilibrium and may show an overall increased mass transfer rate when compared to the other two systems.

Samples were collected at the outlet in 40 cm^3 volatile organic analysis vials with Teflon® lined lids. To reduce volatilization losses, a rubber stopper was used to hold the collection tubing in the vials. Also the vials were filled such that there was no head space and were refrigerated until analysis which was performed within 7 days.

2.4. Chemical analysis

The effluent samples were analyzed for chlorinated benzene concentration using a Hewlett Packard® 5890 gas chromatograph (GC) equipped with a Hewlett Packard® 5971 mass spectrometer detector (MS). Also this system utilized a PTA-30 autosampler and a column being Phenomenex® ZB-624 30 m length by 0.25 mm diameter. The system was controlled by HPChemStation® software. A Tekmar® liquid solid sample concentrator (LSC-2) purge and trap with a purge flow of 40 mL/min was used due to the nature of volatile organics. The analysis was conducted according to the US EPA Method 8260A [12] at initial temperature of 45 °C for 2 min, followed by a ramp to 110 °C at a rate of 6 °C/min, a ramp of 12 °C/min to 210 °C, and hold at the last temperature for 5 min. The flow rate to the MS was 1.0 mL/min with an initial solvent delay of 4 min. Standard curves were prepared and all standards had a correlation coefficient greater than 0.96.

Small cores of the sediments were collected with a 60 mL syringe with the Luerlok® top cut off. Samples were collected in the front, middle and back of the bed, in the direction of the water flow. The cores were cut into vertical thirds. Each subsample was placed in 60 mL amber borosilicate jars with Teflon® lined lids and extracted with methanol under sonication for three hours. The liquid phase was transferred to VOA vials and stored in the dark at 4 °C until analysis. Each sample was extracted three times by the same procedure to obtain all leachable contaminants.

2.5. Experimental flux determination

For the experimental work, the flow from the bed of a contaminant may be calculated as:

$$\text{Flux} = \frac{CQ}{A} \quad (1)$$

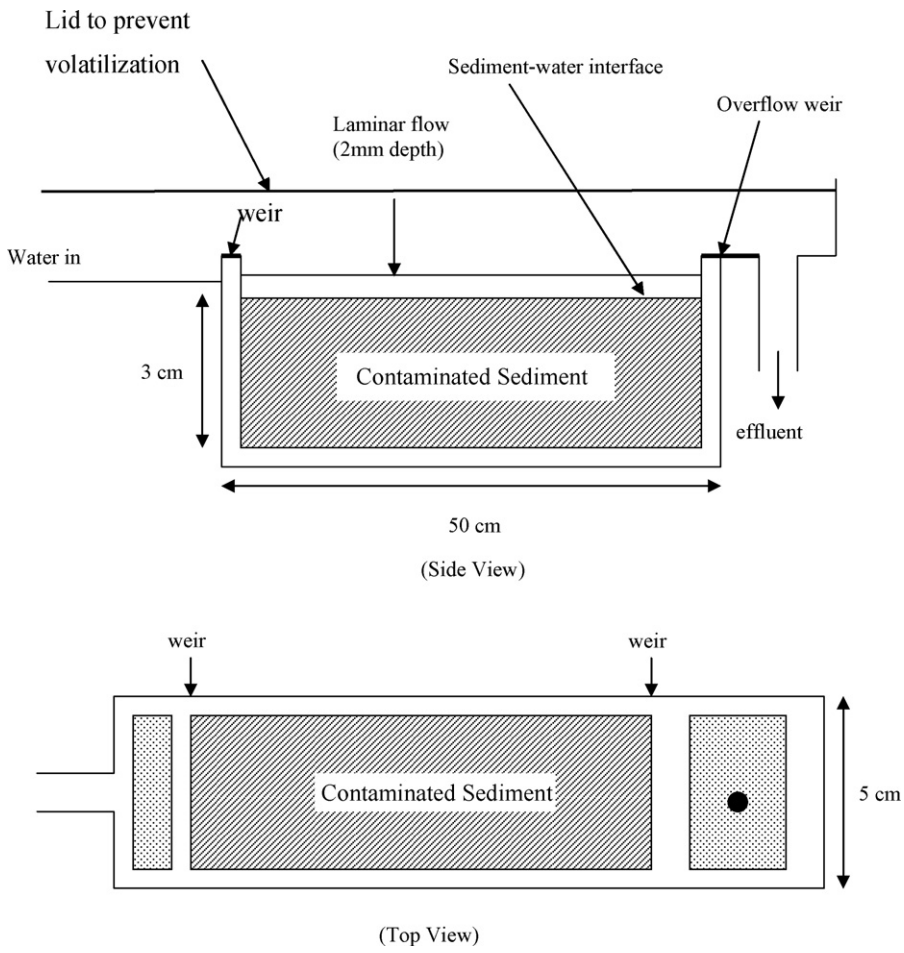

Fig. 1. Sheet flow leaching bed (SFLB).

where C is concentration of chemical in the effluent in mg/L; Q is flow rate (L/h) and A is the area of the bed normal to the flux in cm^2. Flux is given in mg/cm^2 h.

In theory, the effluent mass is calculated by the following equation:

$$M = FA\,\Delta T \tag{2}$$

where M is the mass of contaminant removed from the bed (mg), F is the calculated flux rate and A is the area from Eq. (1), and ΔT is the time between sample n and sample $n+1$ in hours.

Studies of single and multiple contaminant flux and removal were performed. 1,3-DCB was used to determine the effect of different flow regimes (fast, slow and cyclic) in the flux rate and the efficiency of a single contaminant (1,3-DCB).

In a real situation it would be very rare to find a single contaminant in field situations. This certainly holds true in the Baton Rouge Bayou area around the site with multiple chlorinated contaminants present. Experiments with multiple contaminants in sediment were conducted to determine the effect of the difference in chemical properties of the contaminant compounds, like solubility, in the partitioning of each component into the water phase. The flux rate patterns were expected to be different than those of a single contaminant due to differences in partition coefficients, solubility and other parameters.

Flux rates for a four contaminant mixture consisting of 1,2 DCB, 1,3-DCB, chlorobenzene (MCB) and trichlorobenzene (TCB) were measured for the fast, slow and cyclic flow regimes over the laboratory contaminated sediment. The multiple contaminant experiment was performed twice with parallel beds.

In the slow flow experiments the initial starting contaminant load for MCB is 20.25 mg/kg, 1,3-DCB starts at 31.47 mg/kg, 1,2-DCB has initial starting concentration 35.21 mg/kg and TCB is 41.13 mg/kg. For the fast flow experiment the MCB initial load was 25.07 mg/kg, 1,3-DCB initial sediment load was 39.74 mg/kg, 1,2-DCB sediment load was 41.99 mg/kg, and TCB was 53.79 mg/kg. For the cyclic flow experimental initial load for MCB was 17.44 mg/kg, 1,3-DCB had initial load of 42.22 mg/kg, the 1,2 isomer was 42.64 mg/kg and TCB started at 53.38 mg/kg. Each chlorobenzene value is the average of four replicates.

2.6. Mathematical model

Based on the simulations in the EQC (equilibrium criterion) model proposed by Mackay et al. [13], it was noted that at steady state level III (steady state condition with input and resistance for inter-media transport between air, water and soil) there were simulations which showed the environmental impact on fate due to the medium of discharge. When chlorobenzene was discharged into air, it had a compartmental (air) residence time of 3 days and most of it (71%) was advected away. If the medium of discharge was water, it had a compartmental residence time of 13 days and 84% of it stays there. An increased residence time indicates a higher exposure to the contaminant and this impact could highly affect the receptor. Also, when chlorobenzene is discharged into soil its residence time is close to 20 days. This is due to slower processes of desorption and dissolution [14].

In a sensitivity analysis, the mass transfer coefficients "profoundly affect the source concentration in the water" [13]. The

adequate estimation of mass transfer coefficients will have a large effect of the model results [15–17]. Thus, in the following discussion, two different models and three different mass transfer coefficient approaches are presented to investigate this observation.

2.6.1. Development of an advection enhanced diffusion model

Assuming a finite flat source with uniform initial concentration and the flux of the contaminant being diffusion driven upwards from this finite flat source a diffusion model was proposed. This model also helps in tracking the diffusive transport of the contaminants between sediment and water compartments. The design of the SFLB was such that the flux at the base of the bed was not a factor. Also the bulk water contaminant concentration was used to calculate the flux. As the water was flowing across the sediment surface, the experimental flow model was advection based at the surface.

Based on the physical flow conditions, "case 2" and "case 4" from Choy and Reible's [6] derivation of this system were tested. Diffusion in a finite layer with three different mass transfer coefficients was used to evaluate which coefficients described more accurately the experimental data. The Choy and Reible [6] "case 2" flux model considers diffusion in a finite layer with uniform initial concentration, zero surface concentration, and zero flux at the base. For the experimental conditions in this work, it can be assumed that the water flow at the surface provides a zero surface concentration. The water is in laminar flow, 2 mm in depth, across the surface of the SFLB. No advection through the sediment component is assumed. The solution for "case 2" surface flux is given below [1]:

$$F = \frac{2D_e C_o}{H_z} \sum_{n=1}^{\infty} \exp\left(\frac{-D_e}{R_f}\alpha_n^2 t\right) \tag{3}$$

where

$$\alpha_n = \frac{\pi}{H_z}\left(\frac{2n-1}{2}\right) \tag{4}$$

Here H_z is the depth (length) of contaminated sediment, C_o is the initial pore water concentration (mass per volume), R_f is the retardation factor, t is time and D_e is the fitted parameter, effective diffusivity (length $^2/t$). There is no explicit mass transfer term.

The "case 4" model is derived for uniform initial concentration and zero flux at the base but it assumes mass transfer at the surface. The flow across the surface of the SFLB is better represented here by the mass transfer at the surface condition. Also as stated previously there is zero flux at the base (which is accounted for by the stainless steel boundary) and the uniform initial concentration is introduced by well mixed laboratory contamination of the sediment. The solution for the "case 4" surface flux is given as [6]:

$$F = \frac{2D_e C_o}{H_z} \sum_{n=1}^{\infty} \exp\left(\frac{-D_e}{R_f}\alpha_n^2 t\right) \sin^2(\alpha_n H_z) \tag{5}$$

where α_n represent the positive roots of:

$$\alpha_n \tan(\alpha_n H_z) = \frac{k_a}{D_e} \tag{6}$$

and k_a is the surface mass transfer coefficient. The laminar flow boundary layer theory yields a k_a, based on Reynolds and Schmidt numbers ($k_a = 0.664 Re^{0.5} Sc^{1/3}[D_e/H_z]$) given in Choy and Reible [1].

In Eq. (5) the explicit mass transfer coefficient k_a has been introduced. Three modifications of k_a were used in Eq. (5) to observe the impact of different mass transfer coefficient estimations. One such modification used for k_a was the k_{thoma} term which was derived by Thoma [18] in order to verify the negligible water side resistance to mass transfer:

$$k_{thoma} = 1.165\left[\frac{QD_w^2}{H^2 LW}\right]^{1/3} \tag{7}$$

where Q is the volumetric flow rate, D_w is the diffusivity of the compound in water, H is the height of the water layer, L is the length of the water layer and W is the width of the water layer. The second modification/substitution used for k_a was $k_a = Q/A$ where Q is the volumetric flow rate and A is the surface area of flux. This modification was to track changes in transport due to flow rate. The third modification was the use of k_a based on the boundary layer theory, identified as k_q ($k_q = 0.664 Re^{0.5} Sc^{1/3}[D_e/H_z]$).

2.6.2. Model analysis

For the model analysis Mathcad 2000® software was used for higher math functions. Two different parameters litK_d (literature based K_d), and expK_d (experimentally determined K_d) were monitored. The solutions based on these two parameters were used to determine the 'average fitted effective diffusivity' in order to calculate the retardation factor.

The sum squared error (SSE) and root mean squared error (RMSE) were calculated as:

$$SSE = \sum (\text{model flux} - \text{experimental flux})^2 \tag{8}$$

$$RMSE = \left(\frac{SSE}{n-1}\right)^{0.5} \tag{9}$$

The smallest value of this RMSE indicated the best fit for the model. The coefficients litK_d and expK_d were utilized as input parameters for the two models proposed by Choy and Reible [6] and the correct fit average effective diffusivity was determined for each coefficient. Multiple simulations were run to yield a case 2 expK_d and case 2 litK_d. For the case 4 model, three boundary conditions being k_{thoma}, $k_a = Q/A$, k_q were used to determine the literature based and the experimental based K_d. The K_d value reported in literature can vary as much as an order of magnitude. The average literature based (Table 2) and experimental K_d were within the same order of magnitude and no significant difference was found. Given this similitude, one "case 2" K_d and three "case 4" K_d (one per each boundary condition) were used to determine the four flux model solutions, based on the literature based K_d values.

2.6.3. System performance predictors

Effective diffusivity and related tortuosity were the system performance predictors that were examined in this study. The flow rates examined were with fast flow, slow flow and cyclic flow regimes. The effective diffusivity can be modified by the sediment characteristics such as porosity, geometry of the grains and hence, the tortuosity of the media and the resulting concentration gradient of the contaminant [19–22].

The four flux models (one "case 2" and three "case 4") that were determined were fitted to the fast flow regime and the average effective fitted diffusivity was determined for all four runs for both single and multiple contaminants. The following equation relating effective diffusivity to diffusivity in water was utilized:

$$D_e = D_w \frac{\varepsilon}{\tau} \tag{10}$$

D_w is the diffusivity of pure compound in water, ε is the porosity and τ is tortuosity. The effective diffusivity derived for the model was used to estimate the tortuosity. The statistical best fit for the model solutions was under the fast flow regime; so

Table 2
Inputs used for the flux model. The sources of the parameters are indicated.

Parameter	Symbol	Value	Reference
Porosity	ε	0.53	Lab determined
Molecular diffusivity	D_w	9.09×10^{-6} cm^2/s (MCB) 8.33×10^{-6} cm^2/s (DCB) 7.57×10^{-6} cm^2/s (TCB)	[17]
Effective diffusivity	D_e	$D_w\varepsilon^{4/3}$	[11,17]
Length bed	L	50 cm	Lab determined
Volumetric flow rate	Q	50–150 mL/h	Lab determined Varied by experiment
Initial soil load	W	10–15 mg/kg	Lab measured
Bulk density	ρ_b	1.05–1.08	Lab determined
Particle density	ρ_p	2.47–2.74	Lab determined
Retardation factor	R_f	$\varepsilon + \rho_b K_d$	[6,19]
Water side resistance	k_q	$0.664\mathrm{Re}^{0.5}\mathrm{Sc}^{1/3}(D_e/H_z)$	[6] (Re = Reynolds and Sc = Schmidt numbers)
Partition coefficient	K_d	$K_{oc}f_{oc}$	Calculated from literature data [19] and measured in laboratory.
Area of bed	A	258.054 cm^2	Lab determined
Width of bed	W	5.08 cm	Lab determined
Height of soil	H_z	3 cm	Lab determined
Octanol/water partition coefficient	$\log K_{ow}$	2.71–2.98 (MCB) 3.38–3.60 (1,3DCB) 3.38–3.55 (1,2DCB) 4.10 (TCB)	[19] [19] [19] [17]
Organic carbon partition coefficient	$\log K_{oc}$	2.46 (MCB), 3.09 (1,3DCB) 3.12 (1,2DCB) 3.69 (TCB)	[17] [19] [19] [17]
Fraction organic carbon	f_{oc}	0.00213	[19]

MCB = chlorobenzene; 1,3DCB = 1,3-dichlorobenzene; TCB = 1,2,4-trichlorobenzene; 1,2DCB = 1,2-dichlorobenzene (1,2-DCB).

the data under the fast flow regime were used to determine the average tortuosity. Average tortuosity is then used as the system constant to predict flux because it is related to the sediment and the leaching bed apparatus. The mean tortuosity's effectiveness in predicting mass transport under all flow regimes was tested by comparing the "case 4" solution ($k_a = Q/A$) to the other two flow regimes, cyclic and slow. The tortuosity was back calculated for each contaminant based on the fitted average effective diffusivity for each model. The average and standard deviations of the tortuosities from each of the simulations were calculated to determine the best range of tortuosities to describe the SFLB set up. This range of tortuosities (high and low) was then substituted in the "case 4" model to predict the range of expected fluxes under cyclic and slow flow conditions. A similar methodology was used for diffusivity.

3. Results and discussion

3.1. Sediment characteristics for single contaminant chlorinated benzene studies

Results of the analysis performed by the Agronomy Laboratory at LSU of the sediment samples obtained in the sites PPI-1–5 are presented in Table 1. The variations on pH (7.0 ± 0.7), organic matter (OM; below 0.6%), a ratio of Ca:Mg (9.0 ± 4.0), and other parameters from the sediment samples show that with exception of PPI-1, the properties of the sediments are fairly similar, indicating a relatively homogeneous surficial sediments at the site. The organic matter (OM) is used to calculate the fraction of organic carbon (f_{oc}), which is used in the models to get K_d, the estimated partition coefficient. The average OM was calculated to be 0.33%. The average f_{oc} was calculated to be 0.00213 and was used to establish the starting value for the calculation of K_d.

3.2. Experimental measurements for 1,3-dichlorobenzene (1,3-DCB)

3.2.1. Initial contaminant load

The target contaminant load was in the range of 10–15 mg/kg after the sediment transfer and mixing. Actual values of contaminant loading in the various cells were 10.4 mg/kg for the slow flow regime, 13.0 mg/kg for the fast flow regime, and 13.8 mg/kg for cyclic flow regime. Although all the loads were within the target range, variability was observed due to the heterogeneity of the media.

3.2.2. Contaminant flux

The slow and fast flow regimes for 1,3-DCB follow a similar pattern of exponential decay (Figs. 2 and 3). Comparison of the results of the flux profiles for the fast (Fig. 3) and cyclic (Fig. 4) flow regimes

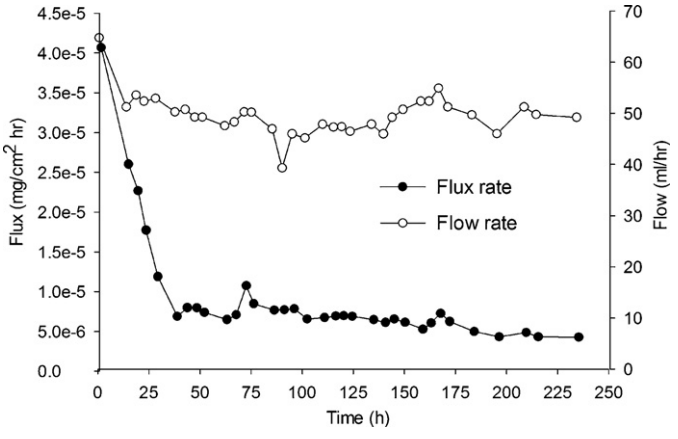

Fig. 2. 1,3-DCB single contaminant flux under slow flow rate.

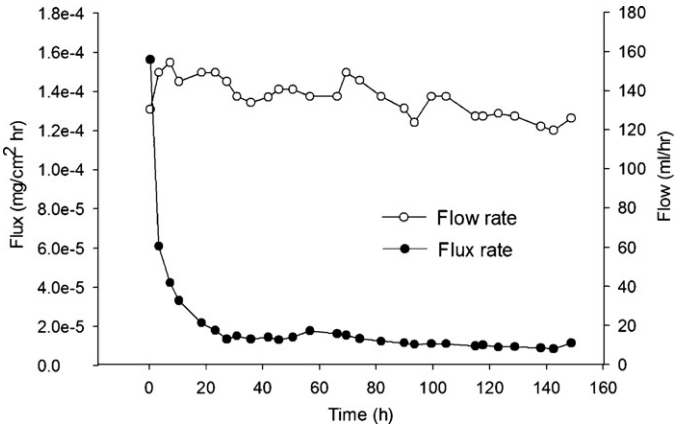

Fig. 3. 1,3-DCB single contaminant flux under fast flow rate.

show that with cyclic flow rates, the contaminant flux presents higher spikes when compared to the fast flow rate. The flux of the contaminant is faster initially for the fast flow regime, but the observed final effluent mass is higher for the cyclic flow regime. These results coincide with other authors [23,24] that found that in higher inflow concentrations, contaminants in the sediments tend to seep to the water at a higher rate than with low inflows. The flow rate directly affects the concentration due to the advective dependence of desorption and dissolution.

Due to the natural cyclic rainfall events scaled and modeled here for Baton Rouge Bayou, this higher rate may increase the flux of chlorinated benzenes. Also, this result suggests that an increase in the flux of chlorinated benzenes into the water due to rainfall events should be included in a mathematical model of the system.

3.2.3. Multiple contaminant studies

In mixture of contaminants studies, the individual component flux rates vary under different flow regimes although the results show overall behavioral similarity (Figs. 5–7). As in the case of the single contaminant, spikes in flux rates were observed for multiple compounds in cyclic flow simulations. After a time of about 4–8 h the flux rates returned steady state.

An exponential decay of the flux, typical of diffusion curves [25] was observed in all the flow regimes. For all three pumping regimes, the fast flow system appears to be the most effective at loss of contaminants to the water column followed by the cyclic rate results. However, it was found that a higher initial sediment loading for the fast flow regime beds may more appropriately explain the higher observed flux rate, coinciding with the observations of other

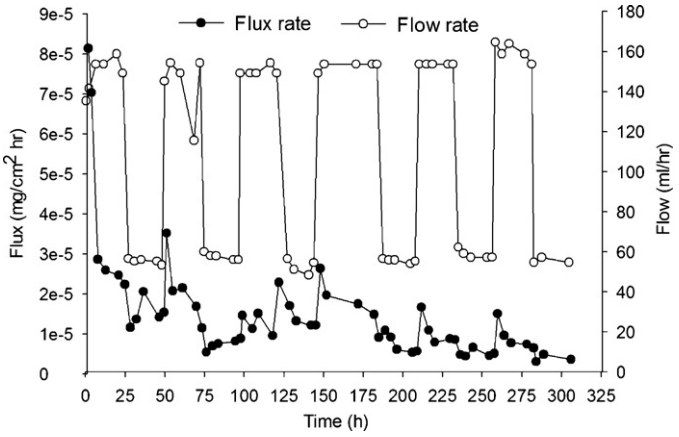

Fig. 4. 1,3-DCB single contaminant flux under cyclic flow rate.

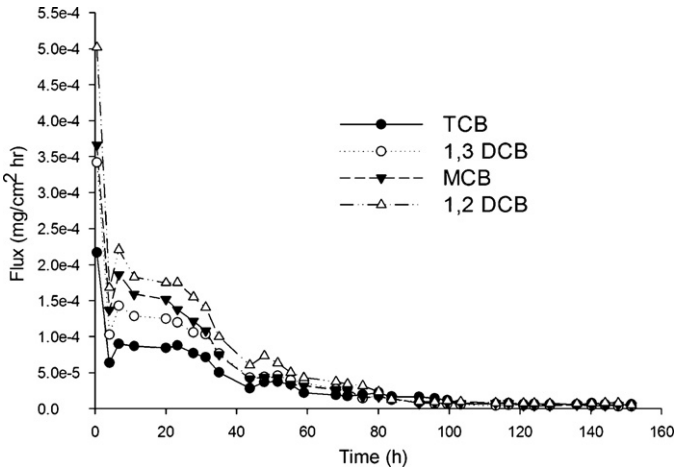

Fig. 5. Contaminant mixture flux under slow flow.

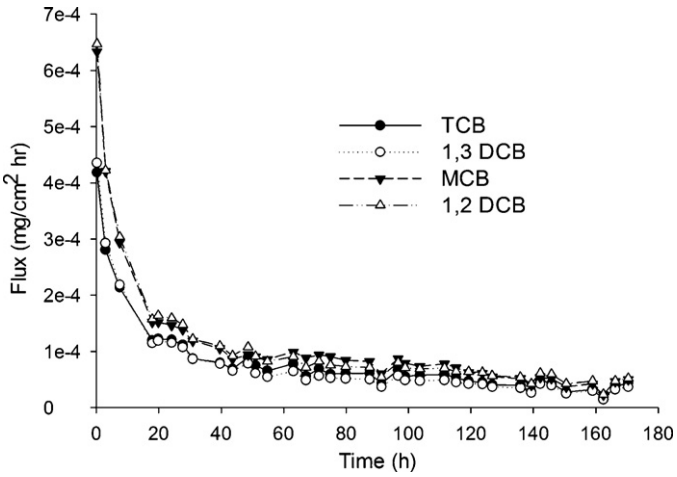

Fig. 6. Contaminant mixture flux under fast flow.

authors [26,27] of a high flux in the initial desorption phases and a lower desorption afterwards. All the experiments indicate that dissolution and desorption is a slow process. This was expected due to the high sorptive capacity of most sediments in comparison to the water solubility of chlorinated benzenes, the solubility limit and critical loading of contaminated sediment [14,28]. The

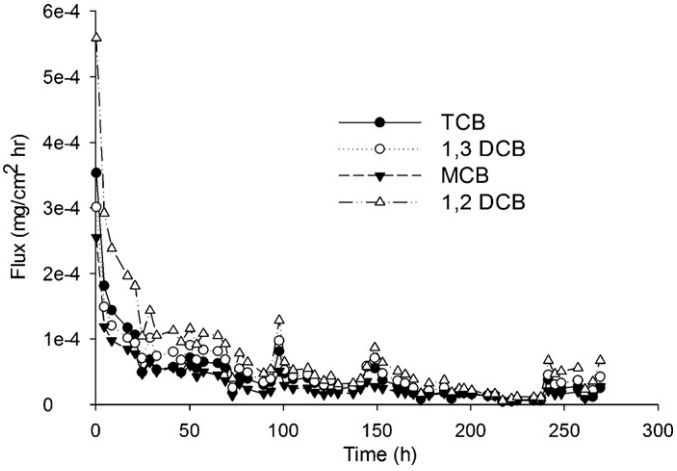

Fig. 7. Contaminant mixture flux under cyclic flow.

experimental results were used as the basis for the development of the diffusion models.

3.3. Modeling results

The input variables used in the models are presented in Table 2. These variables were obtained experimentally or from the literature. With these input data and model results, the model derived flux and experimental flux profiles for 1,3-DCB as the sole contaminant showed no significant differences.

Similarly the mathematical models were fitted to the individual compounds within a multiple contaminant mixture under fast flow conditions. A slight overestimate of the flux was observed with the model, although there was no significant difference between the model and experimental flux, further indicating that the model selected was appropriate for the laboratory scale system.

Table 3 presents the fitted average effective diffusivity for all four model simulations, being "case 2" and "case 4" with different estimates for k_a (mass transfer coefficient). A comparison between the correlation coefficients and the RMSEs indicate that the models are adequate. The four fast flow simulations were used to determine predictive average tortuosity, τ (13 ± 7) and predictive average diffusivity D_e (47×10^{-8} cm^2/s $\pm$ 29×10^{-8} cm^2/s). These two parameters were tested for predicting flux rates under the other two flow regimes (slow and cyclic).

3.3.1. Tortuosity (τ) as a system descriptor

The models are not significantly different from each other and provide a reasonable approximation of the flux. Tortuosity was found to be a good predictor of the flux, although a slight overestimation was observed in all flow regimes. Two examples of the predicted and experimental flux at cyclic and slow flow regimes for 1,3-DCB as single contaminant and as part of a mixture are shown in Figs. 8 and 9.

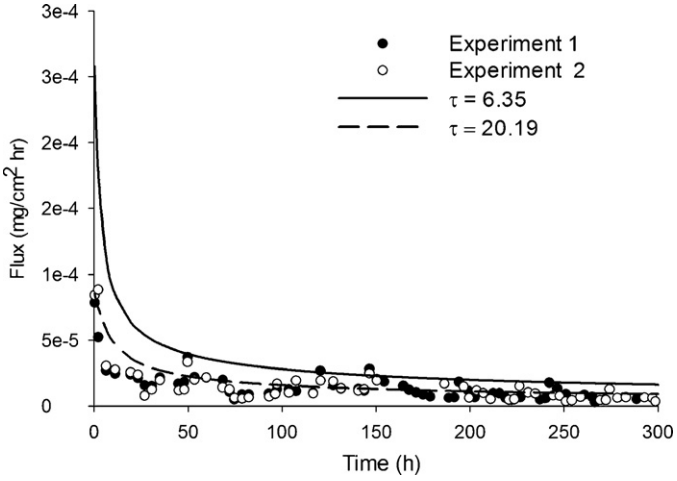

Fig. 8. Tortuosity (τ) as system predictor for 1,3-DCB single contaminant under cyclic flow.

The observed effective diffusivity (Table 3) was compared with the diffusivity calculated with Eq. (6) based on the two τ values under both cyclic and slow flow regimes (Table 4). The predicted coefficients are in the same order of magnitude as the coefficients obtained experimentally, supporting that τ can be used to describe the contaminant transport. These results concur with other authors [20,21] that consider tortuosity an important parameter to describe the mass transfer of organic contaminants between sediment and water.

3.3.2. Effective diffusivity, D_e, as a system predictor

The effective diffusivities for cycle flow slightly overestimated the flux rates of 1,3-DCB as a single contaminant and

Table 3
Summary for calculation of average D_e and tortuosity for system descriptors.

	Fit D_e (10^{-8} cm^2/s)	RMSE (mg/cm^2 h)	τ	Correlation coefficient r
Single MCB fast				
Case 2	20.00 ± 0.22	2.20E−05	24.36	0.862
Case 4, k_q	30.90 ± 0.28	1.62E−05	15.77	0.891
Case 4, k_{thoma}	35.85 ± 0.22	1.53E−05	13.59	0.895
Case 4, Q/A	30.10 ± 0.20	1.57E−05	16.21	0.878
Mixture MCB fast				
Case 2	17.05 ± 0.23	1.92E−05	28.58	0.990
Case 4, k_q	23.55 ± 0.15	1.38E−05	20.69	0.995
Case 4, k_{thoma}	25.06 ± 0.18	1.52E−05	19.44	0.994
Case 4, Q/A	23.19 ± 0.15	1.35E−05	21.01	0.995
Mixture 1,2-DCB fast				
Case 2	46.28 ± 0.15	2.00E−05	9.65	0.993
Case 4, k_q	63.95 ± 0.18	1.48E−05	6.98	0.996
Case 4, k_{thoma}	67.70 ± 0.18	1.65E−05	6.60	0.996
Case 4, Q/A	62.56 ± 0.15	1.42E−05	7.14	0.997
Single 1,3-DCB fast				
Case 2	31.75 ± 0.25	1.81E−05	14.06	0.895
Case 4, k_q	23.10 ± 0.18	7.77E−05	19.32	0.961
Case 4, k_{thoma}	40.00 ± 0.19	1.73E−05	11.16	0.993
Case 4, Q/A	31.10 ± 0.22	1.16E−05	14.36	0.909
Mixture 1,3-DCB fast				
Case 2	28.95 ± 0.18	1.72E−05	15.43	0.995
Case 4, k_q	39.64 ± 0.15	1.63E−05	11.26	0.995
Case 4, k_{thoma}	42.02 ± 0.19	1.71E−05	10.63	0.995
Case 4, Q/A	38.80 ± 0.14	1.59E−05	11.51	0.995
Mixture TCB fast				
Case 2	77.81 ± 0.18	1.52E−05	5.21	0.992
Case 4, k_q	109.75 ± 0.15	1.67E−05	3.70	0.990
Case 4, k_{thoma}	111.30 ± 0.12	1.67E−05	3.65	0.990
Case 4, Q/A	102.50 ± 0.20	1.61E−05	3.96	0.989

Table 4
Model comparison for slow and cyclic flow regimes with tortuosity (τ) as predictor.

	D_e (10^{-7} cm^2/s)	RMSE (mg/cm^2 h)	Correlation coefficient r	D_e (10^{-7} cm^2/s)	RMSE (mg/cm^2 h)	Correlation coefficient r
Slow flow		τ = 6.35			τ = 20.19	
MCB-single	7.7	9.7×10^5	0.968	2.4	2.1×10^5	0.991
1,3DCB-single	7.0	2.6×10^5	0.923	2.2	6.2×10^6	0.959
MCB in mix	7.7	2.0×10^4	0.906	2.4	5.8×10^5	0.932
1,3DCB in mix	7.0	5.9×10^5	0.927	2.2	4.0×10^5	0.921
1,2DCB in mix	7.0	5.6×10^5	0.941	2.2	6.7×10^5	0.935
TCB in mix	6.4	3.6×10^5	0.905	2.0	3.2×10^5	0.892
Cyclic flow		τ = 6.35			τ = 20.19	
MCB-single	7.7	9.1×10^5	0.934	2.4	2.6×10^5	0.904
1,3DCB-single	7.0	3.5×10^5	0.906	2.2	8.3×10^5	0.874
MCB in mix	7.7	2.9×10^5	0.942	2.4	2.2×10^5	0.970
1,3DCB in mix	7.0	1.9×10^5	0.922	2.2	4.1×10^5	0.917
1,2DCB in mix	7.0	2.5×10^5	0.965	2.2	6.4×10^5	0.954
TCB in mix	6.4	3.6×10^5	0.936	2.0	5.5×10^5	0.851

D_e = average effective diffusivity; RMSE= root mean squared error.

Table 5
Model comparison with effective diffusivity (D_e) as predictor.

	τ	RMSE (mg/cm^2 h)	Correlation coefficient r	τ	RMSE (mg/cm^2 h)	Correlation coefficient r
Slow flow		$D_e = 17.97E^{-8}$ cm^2/s			$D_e = 75.1 \times 10^{-8}$ cm^2/s	
MCB-single	27.1	8.7×10^{-6}	0.993	6.485	9.1×10^{-5}	0.971
1,3DCB-single	24.9	4.1×10^{-6}	0.959	5.943	2.8×10^{-5}	0.922
MCB in mix	27.1	4.2×10^{-5}	0.937	6.485	2.0×10^{-4}	0.906
1,3DCB in mix	24.9	4.6×10^{-5}	0.919	5.943	6.1×10^{-5}	0.929
1,2DCB in mix	24.9	7.5×10^{-5}	0.932	5.943	6.1×10^{-5}	0.941
TCB in mix	22.6	3.4×10^{-5}	0.891	5.401	4.0×10^{-5}	0.907
Cyclic flow		$D_e = 18.0 \times 10^{-8}$ cm^2/s			$D_e = 75.1 \times 10^{-8}$ cm^2/s	
MCB-single	27.1	3.2×10^{-5}	0.885	6.485	8.9×10^{-5}	0.934
1,3DCB-single	24.9	6.8×10^{-6}	0.871	5.943	3.7×10^{-5}	0.906
MCB in mix	27.1	2.6×10^{-5}	0.971	6.485	2.7×10^{-5}	0.944
1,3DCB in mix	24.9	4.5×10^{-5}	0.911	5.943	1.0×10^{-5}	0.922
1,2DCB in mix	24.9	7.1×10^{-5}	0.946	5.943	2.8×10^{-5}	0.964
TCB in mix	22.6	5.7×10^{-5}	0.844	5.401	3.3×10^{-5}	0.946

τ = tortuosity; RMSE = root mean squared error.

underestimated the same component in a mixture of contaminants. However for the component MCB in a mixture the flux rates were predicted well by the effective diffusivity.

Using Eq. (6) a new τ was calculated based on two previous values of effective diffusivity which could be used for both slow flow and cyclic flow regimes. The results are presented in Table 5. The predicted models are in the same order as that of the original fitted models based on the RMSE. Also the correlation coefficients are similar further strengthening the use of effective diffusivity as a system predictor and descriptor for modeling contaminant transport in this system.

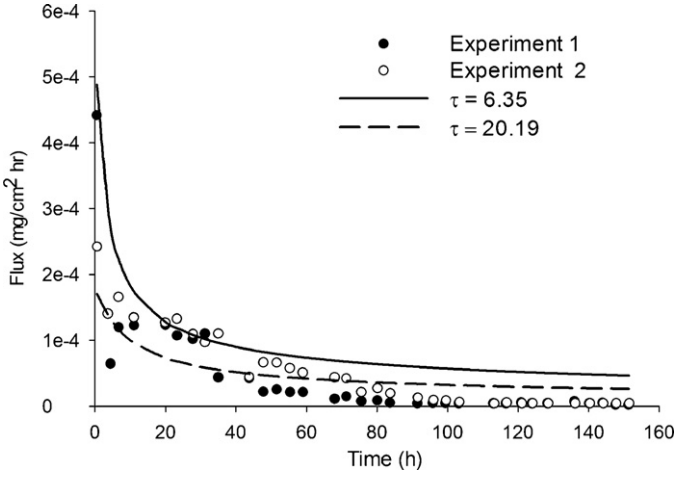

Fig. 9. Tortuosity (τ) as system predictor for 1,3-DCB in mixture under slow flow.

4. Conclusions

For the single contaminant studies utilizing 1,3-DCB the fast and slow flow regimes appear to follow the same trend of exponential decay and the cyclic study demonstrates spikes of higher flux when the flow rate changes yielding a higher overall average flux rate. Thus, natural rainfall events in Baton Rouge Bayou/Devil's Swamp may show higher flux rates of lower chlorinated benzenes than would be expected in steady state systems.

Because natural systems rarely contain one pollutant, studies were performed utilizing four components: chlorobenzene (MCB), 1,2-dichlorobenzene, (1,2-DCB) 1,3-dichlorobenzene (1,3-DCB), and 1,2,4-trichlorobenzene (TCB). The individual component flux rates are shown to vary at all three flow regimes, slow, fast, and cyclic as each compound partitions into the water phase differently due to differences in chemical properties such as the water/octanol partition coefficient (K_{ow}) and solubility. Although the flux showed overall behavioral similarity for all components in a mixture, it should be noted that flux rates for each component in the mixture, under all three pumping regimes, indicated that the fast flow system appears to yield the highest transfer to the water column followed by the cyclic rate. However, fast flow cells had a higher initial sediment load which may explain the higher observed flux rate.

Mathematical modeling studies indicate that flux of contaminants from sediment beds can be quantified and predicted by relatively simple diffusion models. An exponential decay curve is

clearly present in the fast flow experiments and the models fit the experimental data adequately. Under this flow rate, there was no significant difference in the models to adequately predict the diffusive flux of contaminants from surface sediments. The slow and cyclic flow flux could be reasonably predicted with the system descriptors of average tortuosity, τ, and an average effective diffusivity, D_e. Tortuosity is easier to implement and could be used to provide a simple system descriptor for chemical flux rate prediction.

The predictive tortuosities are higher than predicted by the porosity to the 4/3 power and may be more representative of the multiple processes in the experimental sediment system. The RMSE and correlation coefficient demonstrates there is no significant difference between the model cases and very little difference was seen between the uses of experimentally determined parameters or literature based approximations. In the system studied, published diffusion models can be calibrated to adequately describe contaminant movement. Although there was no significant difference between the boundary condition of mass transfer at the surface and the boundary condition of zero surface concentration, the physical process appears to modeled best by the mass transfer coefficient equal to the flow rate over the area. More importantly, it was demonstrated that these models can be effective with minimal experimental determination of input parameters (bulk density, particle density and sediment load), instead relying on fundamental basic parameters such as diffusivity and tortuosity.

In this research, local equilibrium was assumed and the diffusion models of Choy and Reible [1] adequately described the behavior of chlorinated benzenes in SFLBs. Further, the results support the use of equilibrium partitioning models [1] for chlorinated benzene transport at the PPI site in these sediment–surface water systems.

References

[1] W.D. Constant, J.H. Pardue, R.D. Delaune, K. Blanchard, G.A. Breitenbeck, Enhancement of in situ microbial degradation of chlorinated organic waste at the Petro Processors Superfund site, Environ. Prog. 14 (1995) 51–60.

[2] P.B. Jones, R.R. Kommalapati, W.D. Constant, Phytobuffering of lower chlorinated benzene contamination via willows at the PPI Superfund site, J. Hazard. Subst. Res. 3 (2001) 1–17.

[3] K.S. Jørgensen, J.M. Salminen, K. Björklöf, Monitored natural attenuation, in: Bioremediation, Humana Press, 2010, p. 217.

[4] USEPA, Research advances monitored natural attenuation (MNA) techniques for effective site cleanup, L.R. Program, 2007, pp. 1–2, http://www.epa.gov/research/npd/pdfs/lrp-factsheet_mna.pdf.

[5] J.T. Wilson, Monitored natural attenuation of chlorinated solvent plumes, in: H.F. Stroo, C.H. Ward (Eds.), In Situ Remediation of Chlorinated Solvent Plumes, Springer, New York, 2010, pp. 325–355.

[6] B. Choy, D.D. Reible, Diffusion Models of Environmental Transport, CRC, 2000.

[7] S.G. Pavlostathis, M.T. Prytula, Kinetics of the sequential microbial reductive dechlorination of hexachlorobenzene, Environ. Sci. Technol. 34 (2000) 4001–4009.

[8] A. Chaves, D. Shea, D. Danehower, Analysis of chlorothalonil and degradation products in soil and water by GC/MS and LC/MS, Chemosphere 71 (2008) 629–638.

[9] D. Hu, K. Henderson, J. Coats, Fate of transformation products of synthetic chemicals, in: A. Boxall (Ed.), Transformation Products of Synthetic Chemicals in the Environment, 2009, pp. 103–120.

[10] E. Björklund, B. Styrishave, G.G. Anskjær, M. Hansen, B. Halling-Sørensen, Dichlobenil and 2,6-dichlorobenzamide (BAM) in the environment: what are the risks to humans and biota? Sci. Total Environ. 409 (2011) 3732–3739.

[11] J.R. Welty, C.E. Wicks, G. Rorrer, R.E. Wilson, Fundamentals of Momentum, Heat, and Mass Transfer, John Wiley & Sons, 2009.

[12] USEPA, Test Methods for Evaluating Solid Waste, Physical/Chemical Methods, SW-846, 3rd edition, SW8463C, 1992, p. 771.

[13] D. Mackay, A. Di Guardo, S. Paterson, G. Kicsi, C.E. Cowan, D.M. Kane, Assessment of chemical fate in the environment using evaluative, regional and local scale models: Illustrative application to chlorobenzene and linear alkylbenzene sulfonates, Environ. Toxicol. Chem. 15 (1996) 1638–1648.

[14] T.E.M. ten Hulscher, B.A. Vrind, P.C.M. van Noort, H.A.J. Govers, Temperature effects on very slow desorption of native chlorobenzenes from sediment to water, Environ. Toxicol. Chem. 23 (2004) 1634–1639.

[15] J. Go, D.J. Lampert, J.A. Stegemann, D.D. Reible, Predicting contaminant fate and transport in sediment caps: Mathematical modelling approaches, Appl. Geochem. 24 (2009) 1347–1353.

[16] D.F. Pope, S.D. Acree, H. Levine, S. Mangion, J. Van Ee, K. Hurt, B. Wilson, D.S. Burden, Performance Monitoring of MNA Remedies for VOCs in Ground Water, USEPA, 2004, 92 pp.

[17] L.J. Thibodeaux, Environmental Chemodynamics: Movement of Chemicals in Air, Water, and Soil, Wiley-Interscience, 1996.

[18] G.J. Thoma, Studies on diffusive transport of hydrophobic organic chemicals in bed sediments, Dissertation, Department of Chemical Engineering, Louisiana State University, Baton Rouge, Louisiana, 1994, 196 pp.

[19] M. Oostrom, M.J. Truex, G.D. Tartakovsky, T.W. Wietsma, Three dimensional simulation of volatile organic compound mass flux from the vadose zone to groundwater, Ground Water Monit. Remediat. 30 (2010) 45–56.

[20] L. Shen, Z. Chen, Critical review of the impact of tortuosity on diffusion, Chem. Eng. Sci. 62 (2007) 3748–3755.

[21] M.P.J. Smit, T. Grotenhuis, H. Bruning, W.H. Rulkens, Modeling desorption kinetics of a persistent organic pollutant from field aged sediment using a bi-disperse particle size distribution, J. Soils Sediments 10 (2010) 119–126.

[22] S.C. Wu, P.M. Gschwend, Sorption kinetics of hydrophobic organic compounds to natural sediments and soils, Environ. Sci. Technol. 20 (1986) 717–725.

[23] S. Hyun, H. Park, M.Y. Ahn, A.R. Zimmerman, C.T. Jafvert, Fluxes of PAHs from coal tar-impacted river sediment under variable seepage rates, Chemosphere 80 (11) (2010) 1261–1267.

[24] D. Kuntz, P. Grathwohl, Comparison of steady-state and transient flow conditions on reactive transport of contaminants in the vadose soil zone, J. Hydrol. 369 (2009) 225–233.

[25] G. Deane, Z. Chroneer, W. Lick, Diffusion and sorption of hexachlorobenzene in sediments and saturated soils, J. Environ. Eng. 125 (1999) 689.

[26] Y. Chai, J.W. Davis, S.A. Saghir, X. Qiu, R.A. Budinsky Jr., M.J. Bartels, Effects of aging and sediment composition on hexachlorobenzene desorption resistance compared to oral bioavailability in rats, Chemosphere 72 (2008) 432–441.

[27] G. Cornelissen, H. Rigterink, P. van Noort, H.A.J. Govers, Slowly and very slowly desorbing organic compounds in sediments exhibit Langmuir type sorption, Environ. Toxicol. Chem. 19 (2000) 1532–1539.

[28] G. Cornelissen, P.C.M. van Noort, J.R. Parsons, H.A.J. Govers, Temperature dependence of slow adsorption and desorption kinetics of organic compounds in sediments, Environ. Sci. Technol. 31 (1997) 454–460.